Article

TRANSACTIONS OF THE INSTITUTE OF MEASUREMENT & CONTROL

Transactions of the Institute of Measurement and Control
2017, Vol. 39(2) 183–193

DOI: 10.1177/0142331215604210
journals.sagepub.com/home/tim
SAGE

A remote sensing image enhancement method using mean filter and unsharp masking in non-subsampled contourlet transform domain

Lu Liu[1], Zhenhong Jia[1], Jie Yang[2] and Nikola Kasabov[3]

Abstract

The intelligibility of an image can be influenced by the pseudo-Gibbs phenomenon, a small dynamic range, low-contrast, blurred edge and noise pollution that occurs in the process of image enhancement. A new remote sensing image enhancement method using mean filter and unsharp masking methods based on non-subsampled contourlet transform (NSCT) in the scope for greyscale images is proposed in this paper. First, the initial image is decomposed into the NSCT domain with a low-frequency sub-band and several high-frequency sub-bands. Secondly, linear transformation is adopted for the coefficients of the low-frequency sub-band. The mean filter is used for the coefficients of the first high-frequency sub-band. Then, all sub-bands were reconstructed into spatial domains using the inverse transformation of NSCT. Finally, unsharp masking was used to enhance the details of the reconstructed image. The experimental results show that the proposed method is superior to other methods in improving image definition, image contrast and enhancing image edges.

Keywords

Image enhancement, mean filter, NSCT, unsharp masking.

Introduction

Various factors blur the visual effect and reduce image contrast during image collection and transmission. Image enhancement is an image-processed method that can improve image quality, enrich information and strengthen the effect of image interpretation and recognition. Existing image enhancement techniques are mainly based on spatial domain and transform domain. Methods based on the spatial domain include direct grey level transformation, spatial filtering and histogram processing (Buades et al., 2005; Cosman et al., 2014; Di and Gao, 2014; Jain, 1989; Thien et al., 2014; Yang et al., 2003). Methods based on the transform domain transform the image from the time domain to the frequency domain and then process the coefficients of the frequency domain to enhance the image. Examples of this method are algorithms based on the Fourier transform (Backstrom, 2014; Hirschmugl and Gough, 2012; Weisstein, 2015), the wavelet transform (Bhadauria and Dewal, 2014; Iqbal et al., 2014; Vijayan M et al., 2014) and the stationary wavelet transform (Demirel and Anbarjafari, 2011). The multi-resolution analytical method, represented by wavelet analysis (Brown, 2000; Gelman et al., 2005), can suppress the noise of the image while enhancing image details. Additionally, it is easy to control the regions and targets to be enhanced. Separable two-dimensional wavelet functions, expanded by one-dimensional functions, can only capture limited directions, so that the directional information of image cannot be easily represented. The non-subsampled wavelet transform (NSWT) (Mallat, 1989) solved the lack of shift-invariance by downsampled wavelet transform, but the resulting image are often not well reserve the details of the original image features neither in the downsampled nor in the non-subsampled wavelet transform domain, the fundamental reason for which is that the wavelet analysis is not the most optimal function representation methods in the two-dimensional space and cannot depict geometry information in the image. The contourlet transform (CT) overcame this defect associated with the wavelet transform (Do and Vetterli, 2002a, 2002b, 2005; Li and Zhanli, 2014; Swaminathan et al., 2013), as it has good expression performance for two-dimensional images, and is convenient and fast. However, CT also has the drawback of lacking the shift-invariance as the wavelet transform because of the downsampling process. Such a drawback can result in

[1]College of Information Science and Engineering, Xinjiang University, Urumqi 830046, China
[2]Institute of Image Processing and Pattern Recognition Shanghai Jiao Tong University, Shanghai 200400, China
[3]Knowledge Engineering and Discovery Research Institute, Auckland University of Technology, Auckland 1020, New Zealand

Corresponding author:
Zhenhong Jia, College of Information Science and Engineering, Xinjiang University, Urumqi 830046, China.
Email: jzhh@xju.edu.cn

production of the pseudo-Gibbs phenomenon around singularities when using the CT in image enhancement (Do and Vetterli, 2002a, 2002b; Yin et al., 2013; Yu, 2012). The translation invariant issued to wavelet threshold denoising can take away the pseudo-Gibbs phenomenon, but its computing efficiency is low. This study attempts to compensate for the pseudo-Gibbs phenomenon using a non-subsampled contourlet transform (NSCT) (Cunha et al., 2005; Da Cunha et al., 2006; Das and Kundu, 2012; Srivastava and Khare, 2015), which can effectively enhance image details and edges, while avoiding the introduction of new noise. Compared with NSWT, NSCT can provide a better restoration of the image and keep better structure detail, but there are large amounts of operational data and hard computational complexity, so it is difficult effectively to use for some applications that have the higher requirements of real time.

The mean filter is a basic spatial filtering method used in image processing and the most familiar application of it is noise reduction (Bin et al., 2011; Kumar, 2013; Li et al., 2014; Liu H et al., 2010; Liu L et al., 2015). A new remote sensing image enhancement method based on NSCT in the scope for greyscale images is proposed in this study, in which mean filtering is applied to the frequency domain for denoising. The details of the method are as follows: first, the initial image was decomposed into the NSCT domain with a low-frequency sub-band, and several high-frequency sub-bands. Secondly, the mean filter was used for the coefficients of the first high-frequency sub-band for denoising. Linear transformation was adopted for the coefficients of the low-frequency sub-band for enhancing contrast. Then, all sub-bands were reconstructed into spatial domains using the inverse transformation of NSCT. Finally, unsharp masking was used to enhance the details and the edge of the reconstructed image. Compared with the NCST-UM method, the image definition was increased by 31.8% using the proposed method, the grey mean was increased by 3.7% and the image contrast was increased by 24.0% on average.

Theoretical analysis

Non-subsampled contourlet transform (NSCT)

CT is a multi-resolution analysis method for decomposing signals into multi-dimensional and multi-directional detail subbands, allowing for efficient capture of the geometric structure and characteristics of an image. It can achieve better expression of the image than the wavelet transform. Moreover, it is easily adjustable for detecting fine details in any orientation along curvatures, which results in more potential for effective analysis of images. The initial image is decomposed into a series of low- and high-frequency sub-bands on different scales by the Laplacian pyramid (LP) and directional filter bank (DFB) of the CT. This eventually creates multi-resolution, local and multi-direction expressions of the image. However, theoretical analysis of the CT shows that there is a downsampling process in the LP and DBF of the CT. This downsampling produces a pseudo-Gibbs phenomenon around singularities, because it lacks shift-invariance, which weakens the local quality and characteristics of the directional selection, resulting in image distortion in a certain direction.

NSCT is developed on the basis of CT, which not only possesses the multidirection and multi-scale aspects of CT, but also the shift-invariance that CT lacks. NSCT consists of two filter banks, i.e. the non-subsampled pyramid filter bank (NSPFB) and the non-subsampled directional filter bank (NSDFB), as shown in Figure 1(a), which split the 2-D frequency plane in the sub-bands illustrated in Figure 1(b). The NSPFB provides non-subsampled multi-scale decomposition and captures the point discontinuities. The NSDFB provides non-subsampled directional decomposition and links point discontinuities to linear structures. NSCT will more efficiently capture the geometrical characteristics of the image, and noise can be better separated from the weak edge information of the image in the NSCT domain. Therefore, NSCT is widely applied in many fields, for example extraction of image

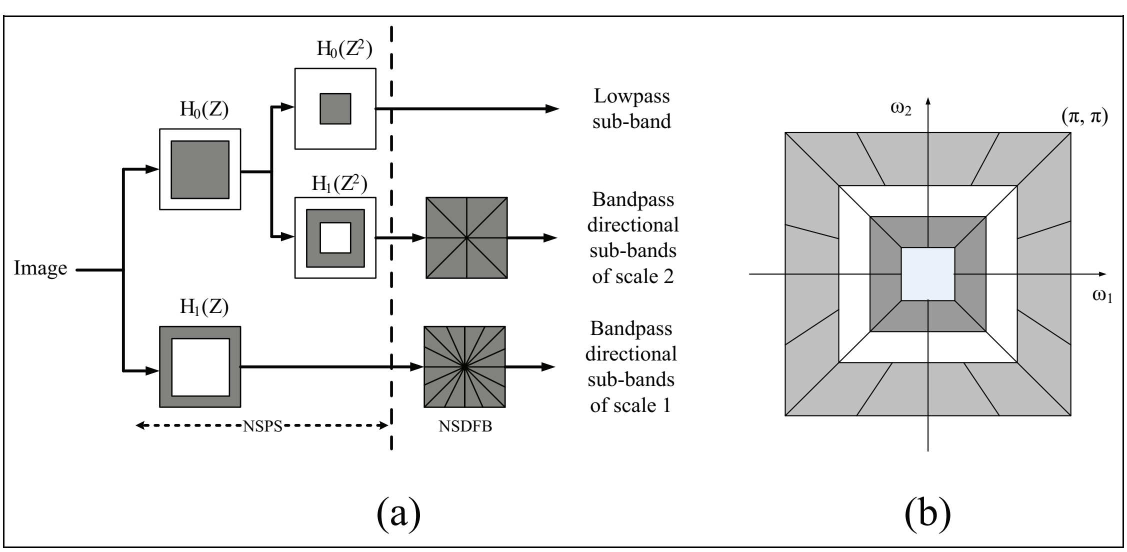

Figure 1. Overall structure of the non-subsampled contourlet transform (NSCT): (a) non-subsampled filter bank structure; (b) the idealized frequency partitioning.

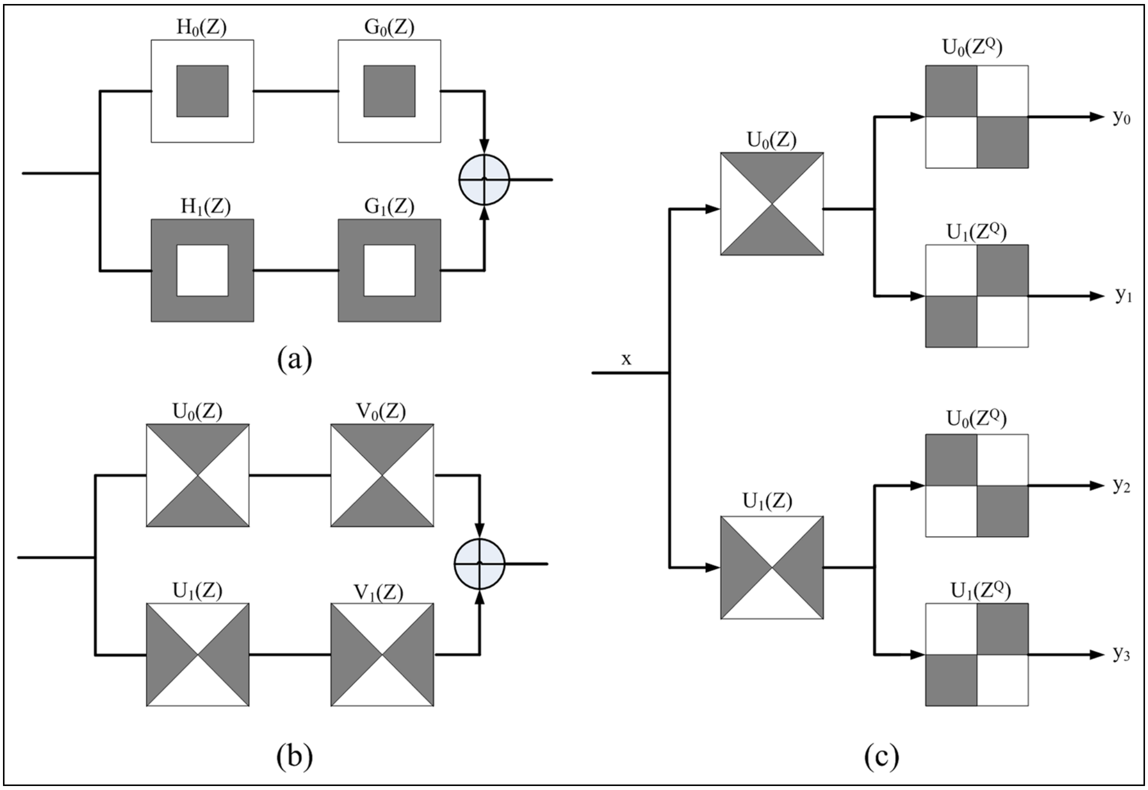

Figure 2. (a) Ideal frequency response of the building block of non-subsampled pyramid filter bank (NSPFB); (b) ideal frequency response of the building block of non-subsampled directional filter bank (NSDFB); (c) four-channel analysis NSDFB structure.

characteristics, image enhancement, image denoising and image fusion. NSCT is used for image enhancement in this study.

The non-subsampled pyramid filter bank (NSPFB). The fundamental building block of NSP is a two-channel filter bank without upsamplers and downsamplers (Ganasala and Kumar, 2014). Figure 2(a) shows the ideal frequency response. The first-stage analysis filters are expressed as $H_k(Z)(k=0,1)$ and the synthesis filters are expressed as $G_k(Z)(k=0,1)$. The perfect reconstruction condition is given as

$$H_0(Z)G_0(Z) + H_1(Z)G_1(Z) = 1 \tag{1}$$

The two-stage decomposition structure of NSPFB is shown in Figure 1(a). By upsampling the filters of the previous stage, the filters for subsequent stages can be acquired. So without additional filter design, it possess the multi-scale property. $H_0(Z)$ and $H_1(Z)$ are first-stage low-pass and band-pass filters, $H_0(Z^2)$ and $H_1(Z^2)$ are second-stage low-pass and band-pass filters.

The non-subsampled directional filter bank (NSDFB). The fundamental building block of NSDFB is a two-channel fan filter bank. Figure 2(b) show the ideal frequency response. The analysis filters are expressed as $U_k(Z)(k=0,1)$ and the synthesis filters are expressed as $V_k(\mathrm{Z})(k=0,1)$. This results in a tree composed of two-channel non-subsampled filter banks by a quincunx matrix given by

$$Q = \begin{bmatrix} 1 & 1 \\ 1 & -1 \end{bmatrix} \tag{2}$$

$U_k(Z^Q)(k=0,1)$ are the second-stage synthesis filters. Four directional sub-bands (y_k, $k=0,1,2,3$) are gained by the two-stage analysis NSDFB in Figure 2(c). The l stage NSDFB can generate 2^l directional sub-bands.

Mean filter

The mean filter algorithm, also called neighbourhood averaging, is a traditional image processing method. For the prevalent white Gaussian noise, mean filters have a better restraining effect compared with a median filter. The mean filter algorithm replaces the value of every pixel in an image with the average of the intensity levels in the neighbourhood that are defined by the filter mask. For example, we choose 3×3 template and the average value at any location (x,y) in the image is the sum of the nine intensity values in the 3×3 neighbourhood centred on (x,y) divided by 9. Letting $z_i, i=1, 2, \ldots, 9$, and denoting these intensities, the average is

$$R = \frac{1}{9}\sum_{i=1}^{9} z_i \tag{3}$$

Although the mean filter method is simple, fast and can effectively reduce noise in images, it also creates blurred edges. To reduce this side effect, the mean filter algorithm is combined with the unsharp masking method in this article.

Unsharp masking

The unsharp masking method (İlk et al., 2011; Kwok and Shi, 2014; Polesel et al., 2000) is an algorithm that is commonly used for edge enhancement. In this method, the edge sharpening is accomplished by subtracting the Laplace filtering component from the original image using the following equation:

$$g(x,y) = f(x,y) + K \times (f(x,y) - f'(x,y)) \tag{4}$$

where $f(x,y)$ represents the original image, $g(x,y)$ represents the enhanced image with unsharp masking method and $f'(x,y)$ represents the artificial vague image, namely the low-pass template.

$$f'(x,y) = \frac{1}{M \times N} \sum_{i=x-(M-1)/2}^{x+(M-1)/2} \sum_{j=y-(N-1)/2}^{y+(N-1)/2} f(i,j) \tag{5}$$

$M \times N$ is the size of the template, generally $M = N$. The equation will produce different effects based on the set value of the enhancement factor K. It can effectively enhance the image edges and detailed information, and accordingly enhance the outline by this method. Nevertheless, the linear unsharp masking method is sensitive to noise. Therefore, the proposed method first reduces the noise in the high-frequency sub-bands, and then increases the coefficients of the high-frequency sub-bands to enhance the edge and details of the image.

The implementation of algorithm

Linear enhancement in low-frequency sub-band

The low-frequency sub-band of NSCT contains plenty of original image information and the noise is filtered, which is the most important step for enlarging the dynamic range of the grey level. To enlarge the contrast effectively, linear stretching is adopted on the basis of the minimum and maximum values of the low-frequency sub-band coefficients, so it can increase the feeling of the administrative levels of the image efficiently. First, we compute the minimum x_{mix} of greyscale value, and the maximum x_{max}, then transform the grey level range from $[x_{mix}, x_{max}]$ to [0, 255] using the linear mapping function:

$$f(x) = 255(x - x_{\min})/(x_{\max} - x_{\min}) \tag{6}$$

Denoising in high-frequency sub-band

Images always include distinct edges, fuzzy edges, a smooth part and some noise. However, the noise is always increased while enhancing the image edges, because noise exists in high-frequency sub-bands as details of the image. The strong edge must be preserved in order to avoid distortion and effectively suppress noise while enhancing the image edges. In this paper, the mean filter is used for denoising the first high-frequency sub-band, leaving the second and third high-frequency sub-bands unprocessed.

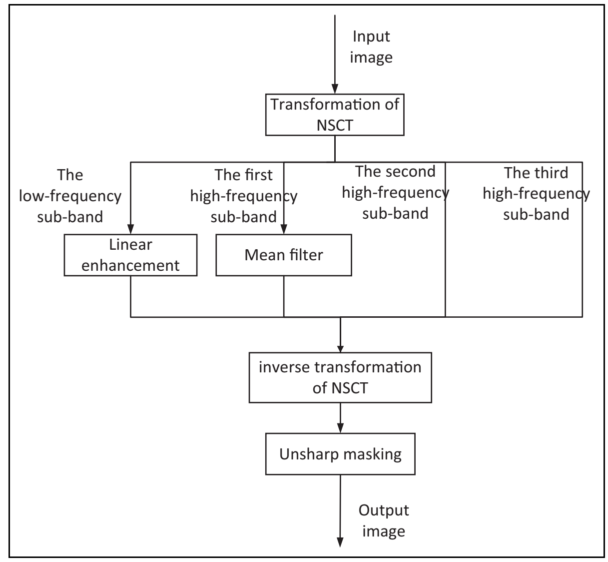

Figure 3. Flowchart of the proposed method.

Steps of the proposed algorithm

1) Decompose the input image using NSCT, obtaining a low-frequency sub-band and several high-frequency sub-bands.
2) Adopt linear stretching using Equation (6) to enhance the contrast of the low-frequency sub-band.
3) For the first high-frequency sub-band, suppress image noise using the mean filter.
4) Reconstruct all coefficients after they are processed using the inverse transformation of NSCT.
5) Obtain the final enhanced image using the unsharp masking method.

Experimental results and analysis

At present, image enhancement evaluation methods are divided into two categories – subjective evaluation and objective evaluation. Subjective evaluation has a strong empirical performance because it judges images from the point of view of the human visual perception. However, it is difficult to simulate the human visual system (HVS) accurately, and the subjective evaluation system based on the HVS can only qualitatively describe the image enhancement, not quantitatively. We adopt both the subjective and objective evaluation methods in order to evaluate the enhanced performance of our proposed image enhancement technique. Definition, contrast, peak signal-to-noise ratio (PSNR) and Q^{AF} are used to evaluate the enhanced image.

Definition reflexes the texture and details of the images, and the higher the definition, the clearer the image is. It is given in the formula:

$$\bar{g} = \frac{1}{M \times N} \sum_{i=1}^{M} \sum_{j=1}^{N} \sqrt{\frac{(\Delta_m x(i,j))^2 + (\Delta_n x(i,j))^2}{2}} \quad (7)$$

where M and N are rows and columns of the image respectively, $\Delta_m x(i,j)$ and $\Delta_n x(i,j)$ represent the differences of direction m and n at location (i,j) of the image, respectively.

Contrast reflects the overall contrast of the images, and the larger the contrast, the higher the overall contrast of the image is. Contrast is calculated by the formula:

$$Con = \frac{VAR}{\left[\frac{1}{M \times N} \sum_{i=1}^{M} \sum_{j=1}^{N} (x(i,j) - \mu_x)^4\right]^{\frac{1}{4}}} \quad (8)$$

where M and N denote the height and width of the image, μ_x is mean of the image, and VAR is variance of the image:

$$VAR = \frac{1}{M \times N} \sum_{i=1}^{M} \sum_{j=1}^{N} (x(i,j) - \mu_x)^2 \quad (9)$$

PSNR is the most commonly used method for evaluating an image objectively. It denotes specific values for the greatest possible power and destructive noise power. The bigger the PSNR, the better the enhancement effect is. PSNR is calculated by the formula:

$$PSNR = 10 \times \lg \frac{L \times L}{MSE} \quad (10)$$

L represents the range of greyscale, generally 255. MSE is mean squared error:

$$MSE = \frac{\sum_{0 \le j \le N} \sum_{0 \le i \le M} (f_{ij} - o_{ij})^2}{M \times N} \quad (11)$$

where f_{ij} and o_{ij} are input image and output image, and M and N denote the height and width of the image.

Edge information preservation values Q^{AF} provide retention of the edge information, expressing the reserved information of the edge strength and direction of images (Xydeas and Petrović, 2000). Q^{AF} is normalization between 0 and 1. $Q^{AF} = 0$ denotes that the edge information of original image is completely lost and $Q^{AF} = 1$ denotes that the edge information of original image are retained integrally. It is defined as:

$$Q^{AF} = \sum_{n=0}^{N} \sum_{m=0}^{M} Q_g^{AF}(n,m) Q_\alpha^{AF}(n,m) \quad (12)$$

$Q_g^{AF}(n,m)$ and $Q_\alpha^{AF}(n,m)$ model perceptual loss of information in the output image F, on the basis of how well the strength and orientation values of a pixel $p(n,m)$ in input image A are represented in the enhancement image F.

$$Q_g^{AF}(n,m) = \frac{\Gamma_g}{1 + e^{K_g^{(G^{AF}(n,m) - \sigma_g)}}} \quad (13)$$

$$Q_\alpha^{AF}(n,m) = \frac{\Gamma_\alpha}{1 + e^{K_\alpha^{(A^{AF}(n,m) - \sigma_\alpha)}}} \quad (14)$$

where Γ_g, K_g, σ_g and Γ_α, K_α, σ_α are contrasts; the relative strength values of $G^{AF}(n,m)$ and orientation values of $A^{AF}(n,m)$ are formed as

$$G^{AF}(n,m) = \begin{cases} \dfrac{g_F(n,m)}{g_A(n,m)}, & if \quad g_A(n,m) > g_F(n,m) \\ \dfrac{g_A(n,m)}{g_F(n,m)}, & otherwise \end{cases} \quad (15)$$

$$A^{AF}(n,m) = \frac{||\alpha_A(n,m) - \alpha_F(n,m)| - \pi/2|}{\pi/2} \quad (16)$$

where

$$g_A(n,m) = \sqrt{s_A^x(n,m)^2 + s_A^y(n,m)^2} \quad (17)$$

$$\alpha_A(n,m) = \tan^{-1}\left(\frac{s_A^y(n,m)}{s_A^x(n,m)}\right) \quad (18)$$

where $s_A{}^x(n,m)$ and $s_A{}^y(n,m)$ are the exports of the horizontal and vertical Sobel edge operator convolved with the corresponding pixels that are centred on each pixel $p_A(n,m)$ of image A, $1 \le n \le N$ and $1 \le m \le M$. M and N denote the height and width of the image.

In this experiment, the proposed method is compared with the histogram equalization method (HE), the CT algorithm (Nezhadarya and Shamsollahi, 2006), the multiscale retinex algorithm (MSR) (Henan et al., 2011), the fuzzy contrast enhancement based on NSCT (NSCT-FU) (Men et al., 2010) and the unsharp masking method based on NSCT (NSCT-UM) (Pu et al., 2014). For the CT and NSCT, we use eight, 16 and 16 directions in the scales.

Figures 4–7 show the visual effect on the image of the six different methods. Image 1 is 256 × 256, image 2 is 140 × 140, image 3 is 556 × 556 and image 4 is 184 × 184, and their greyscale levels are all 256.

The definition and contrast of the image enhanced by the proposed method are higher in the other methods (Table 1). The visual effect of the image enhanced by NSCT-UM is better than CT, MSR and NSCT-FU in Figure 4. Compared with the NSCT-UM method, the proposed method increases the definition of the image by 46.1%, and the contrast is increased by 37.2%. Figure 4 shows that the proposed method has a better visual effect on image 1 than the other enhancement methods.

The image enhancement results of image 2 show that the definition, contrast and PSNR of the proposed method are better than the other methods (Table 2). The Q^{AF} of the image enhanced by NSCT-FU is best, but the definition, the contrast and the PSNR are not a patch on the result by the proposed method. The objective result and visual effect of the NSCT-UM are better than CT, MSR and NSCT-FU. Compared with the NSCT-UM method, the definition of the proposed

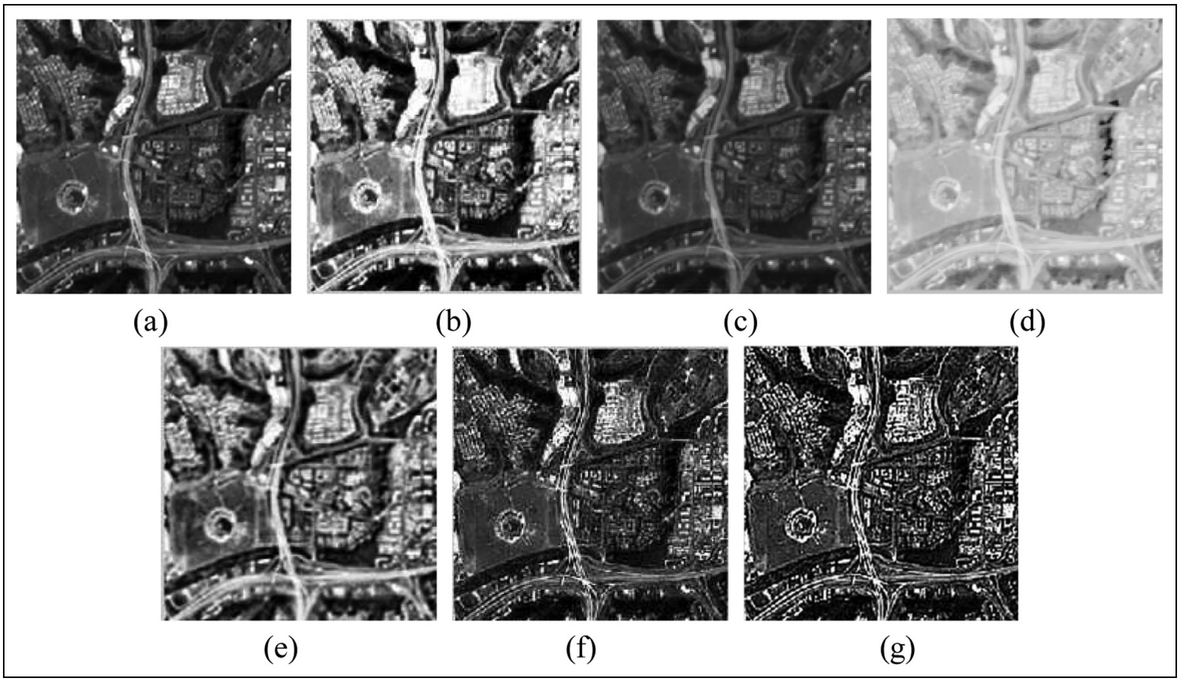

Figure 4. Enhancement results of the six different methods on image 1: (a) original image; (b) image enhanced by histogram equalization (HE); (c) image enhanced by contourlet transform (CT); (d) image enhanced by multiscale retinex algorithm (MSR); (e) image enhanced by the fuzzy contrast enhancement based on non-subsampled contourlet transform (NSCT-FU); (f) image enhanced by the unsharp masking method based on NSCT (NSCT-UM); (g) image enhanced by the proposed method.

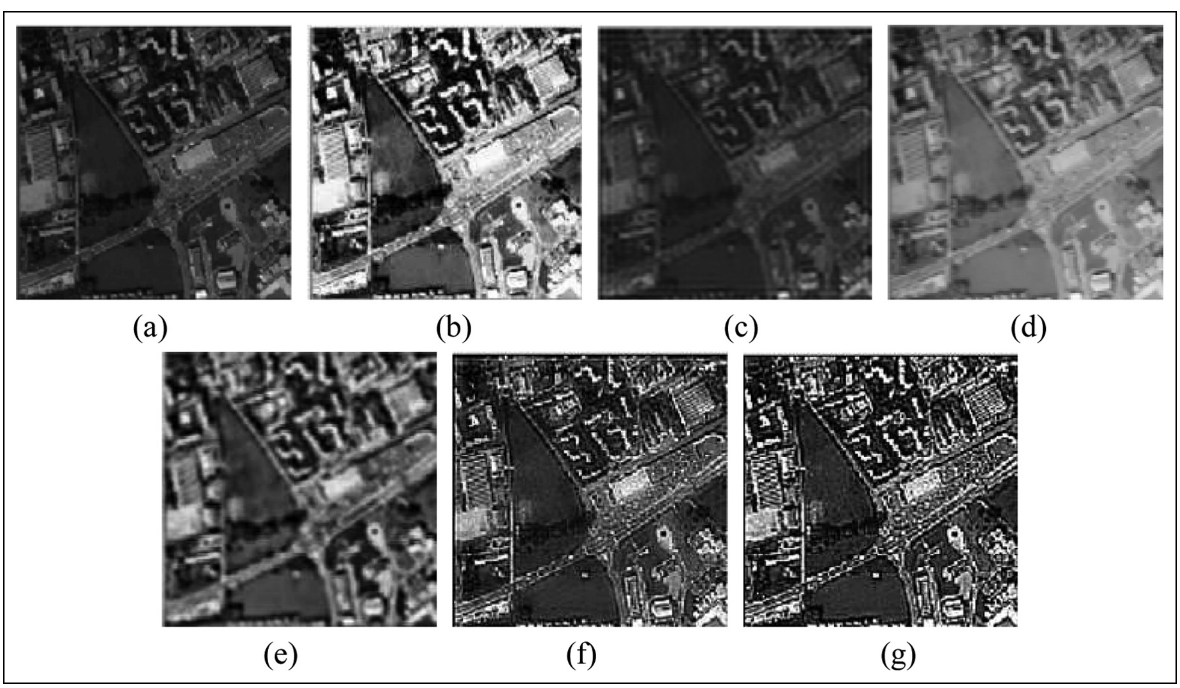

Figure 5. Enhancement results of the six different methods on image 2: (a) original image; (b) image enhanced by histogram equalization (HE); (c) image enhanced by contourlet transform (CT); (d) image enhanced by multiscale retinex algorithm (MSR); (e) image enhanced by the fuzzy contrast enhancement based on non-subsampled contourlet transform (NSCT-FU); (f) image enhanced by the unsharp masking method based on NSCT (NSCT-UM); (g) image enhanced by the proposed method.

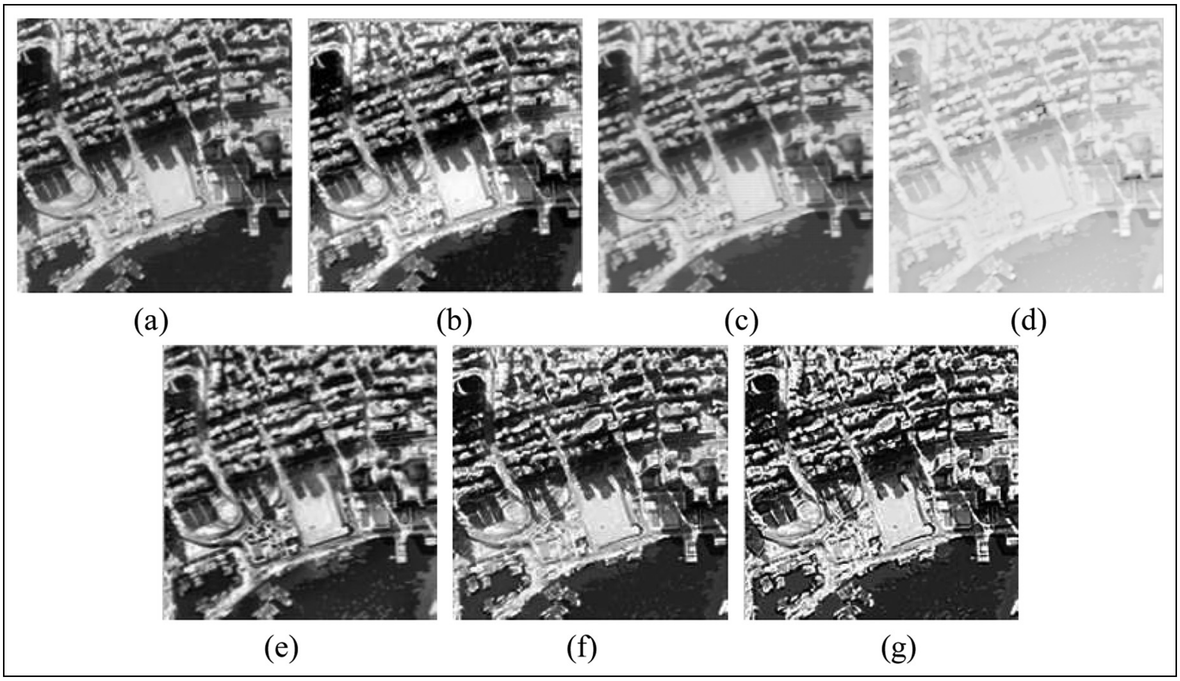

Figure 6. Enhancement results of the six different methods on image 3: (a) original image; (b) image enhanced by histogram equalization (HE); (c) image enhanced by contourlet transform (CT); (d) image enhanced by multiscale retinex algorithm (MSR); (e) image enhanced by the fuzzy contrast enhancement based on non-subsampled contourlet transform (NSCT-FU); (f) image enhanced by the unsharp masking method based on NSCT (NSCT-UM); (g) image enhanced by the proposed method.

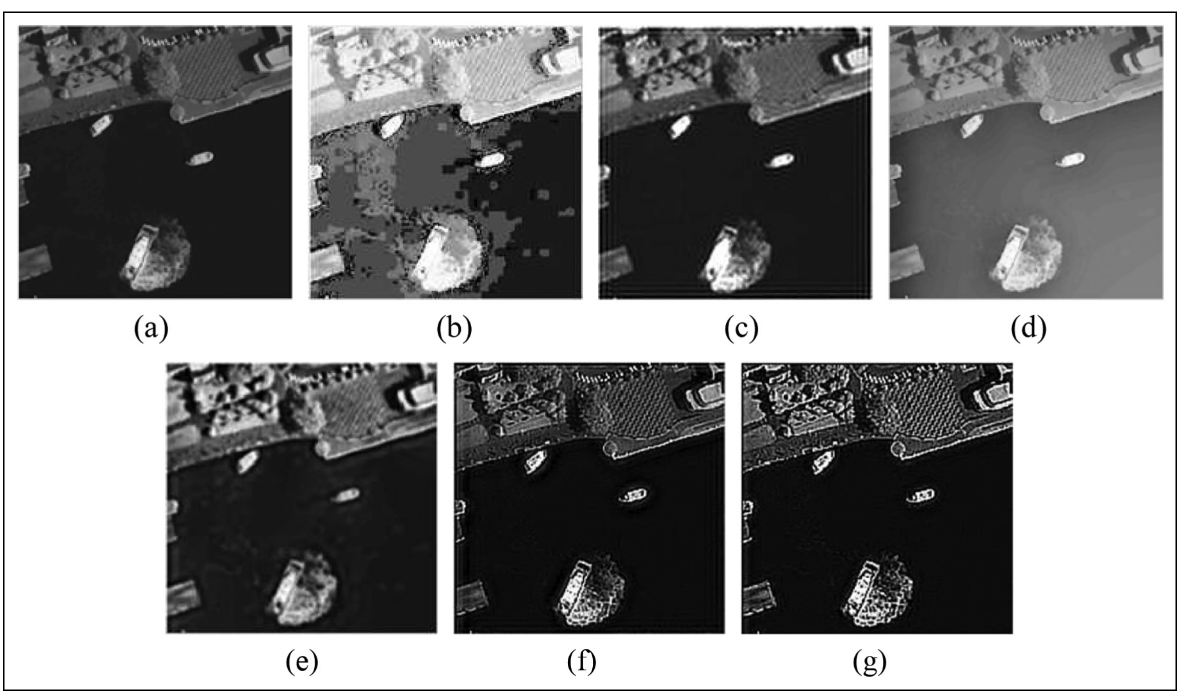

Figure 7. Enhancement results of the six different methods on image 4: (a) original image; (b) image enhanced by histogram equalization (HE); (c) image enhanced by contourlet transform (CT); (d) image enhanced by multiscale retinex algorithm (MSR); (e) image enhanced by the fuzzy contrast enhancement based on non-subsampled contourlet transform (NSCT-FU); (f) image enhanced by the unsharp masking method based on NSCT (NSCT-UM); (g) image enhanced by the proposed method.

Table 1. The objective indicator of the six enhancement algorithms of image 1.

	HE	CT	MSR	NSCT-FU	NSCT-UM	Proposed method
Definition	11.63	22.10	8.98	24.92	21.09	30.82
Contrast	59.59	47.42	15.50	56.27	44.54	61.09
PSNR	25.41	19.06	24.13	14.30	30.75	29.01
Q^{AF}	0.95	0.86	0.059	0.44	0.97	0.52

HE, histogram equalization; CT, contourlet transform; MSR, multiscale retinex algorithm; NSCT-FU, the fuzzy contrast enhancement based on non-subsampled contourlet transform; NSCT-UM, unsharp masking method based on NSCT unsharp masking method based on NSCT; PSNR, peak signal-to-noise ratio.

Table 2. The objective indicator of the six enhancement algorithms of image 2.

	HE	CT	MSR	NSCT-FU	NSCT-UM	Proposed method
Definition	18.66	22.44	21.29	26.18	27.71	39.83
Contrast	64.49	31.62	28.84	43.85	48.97	67.51
PSNR	24.75	22.33	24.13	12.62	25.46	26.14
Q^{AF}	0.10	0.39	0.16	0.90	0.82	0.45

HE, histogram equalization; CT, contourlet transform; MSR, multiscale retinex algorithm; NSCT-FU, the fuzzy contrast enhancement based on non-subsampled contourlet transform; NSCT-UM, unsharp masking method based on NSCT unsharp masking method based on NSCT; PSNR, peak signal-to-noise ratio.

Table 3. The objective indicator of the six enhancement algorithms of image 3.

	HE	CT	MSR	NSCT-FU	NSCT-UM	Proposed method
Definition	4.67	14.82	3.79	12.38	15.94	25.10
Contrast	64.54	84.10	13.89	60.27	65.38	73.98
PSNR	27.73	16.06	24.32	18.84	29.86	28.74
Q^{AF}	0.96	0.74	0.13	0.94	0.96	0.97

HE, histogram equalization; CT, contourlet transform; MSR, multiscale retinex algorithm; NSCT-FU, the fuzzy contrast enhancement based on non-subsampled contourlet transform; NSCT-UM, unsharp masking method based on NSCT unsharp masking method based on NSCT; PSNR, peak signal-to-noise ratio.

Table 4. The objective indicator of the six enhancement algorithms of image 4.

	HE	CT	MSR	NSCT-FU	NSCT-UM	Proposed method
Definition	7.61	11.98	8.63	12.59	12.85	17.39
Contrast	63.88	36.94	21.60	40.90	34.19	42.62
PSNR	24.93	20.37	24.11	18.01	31.36	31.61
Q^{AF}	0.94	0.046	0.007124	0.96	0.018	0.93

HE, histogram equalization; CT, contourlet transform; MSR, multiscale retinex algorithm; NSCT-FU, the fuzzy contrast enhancement based on non-subsampled contourlet transform; NSCT-UM, unsharp masking method based on NSCT unsharp masking method based on NSCT; PSNR, peak signal-to-noise ratio.

method is increased by 43.7%, the contrast is increased by 37.9% and the PSNR is increased by 2.7%. Figure 5 shows that the proposed method has a better visual effect on image 2 than the other enhancement methods.

It is also can be seen that the definition, the contrast and the Q^{AF} of the proposed method are higher than the other methods (Table 3). However, the PSNR of the proposed method are a bit lower than the NSCT-UM method. After using synthesis to analyse the image, the proposed method is better than the other methods. Figures 6 show that the proposed method has a better visual effect on the image than other enhancement methods, with clearer image details and image outline. The definition and the PSNR of the proposed method are higher than the other methods (Table 4). The contrast of the image enhanced by the HE method is the highest in the table, but other indicators are all lower than the

Table 5. The average objective indicator by six methods on 75 images.

	HE	CT	MSR	NSCT-FU	NSCT-UM	Proposed method
Definition	15.07	18.99	13.45	24.43	27.88	37.57
Contrast	64.73	52.71	17.45	49.42	58.52	72.97
PSNR	28.48	23.44	24.47	16.48	29.19	28.71
Q^{AF}	0.62	0.59	0.38	0.68	0.52	0.49

HE, histogram equalization; CT, contourlet transform; MSR, multiscale retinex algorithm; NSCT-FU, the fuzzy contrast enhancement based on non-subsampled contourlet transform; NSCT-UM, unsharp masking method based on NSCT unsharp masking method based on NSCT; PSNR, peak signal-to-noise ratio.

Table 6. The objective indicator of processing different high-frequency sub-band to image 1.

	Processing the first high-frequency sub-band	Processing the second high-frequency sub-band	Processing the third high-frequency sub-band	Processing all high-frequency sub-bands
Definition	30.82	28.76	20.25	14.76
Contrast	61.09	56.46	53.97	45.40
PSNR	29.01	29.27	29.50	30.79
Q^{AF}	0.52	0.87	0.87	0.82

HE, histogram equalization; CT, contourlet transform; MSR, multiscale retinex algorithm; NSCT-FU, the fuzzy contrast enhancement based on non-subsampled contourlet transform; NSCT-UM, unsharp masking method based on NSCT unsharp masking method based on NSCT; PSNR, peak signal-to-noise ratio.

proposed method. It is also can be seen that the Q^{AF} of the NSCT-FU method is the highest in the table, and the Q^{AF} of the proposed method is decreased by 3.1% compared with the NSCT-FU method. Figure 7 also shows that the proposed method has a better visual effect on image 4 than the other enhancement methods.

In order to illustrate applicability of the proposed method, we selected 75 images to experiment with six methods. Compared with NSCT-UM, the average definition of the proposed method increased by 34.8% (Table 5). Furthermore, the average contrast increased by 24.7%, but the average PSNR decreased by 1.6% and the average Q^{AF} decreased by 5.7%.

It is worth mentioning why only the first high-frequency sub-band was mean-filtered. In order to achieve the optimal effect of image enhancement, we processed different high-frequency sub-bands of image 1 using the mean filter (Table 6, Figure 8). The PSNR is the best at processing all high-frequency sub-bands, but it sacrifices image definition and contrast in the process. According Table 5, we can find the PSNR and the Q^{AF} of the proposed method are a little lower than the NSCT-UM method among the five indicators. So the mean filter is not a perfect denoising algorithm, as it can obscure images when denoising. Maybe a non-local mean filter can achieve a better effect. After analysing by synthesis, the enhanced result of processing the first high-frequency sub-band is best.

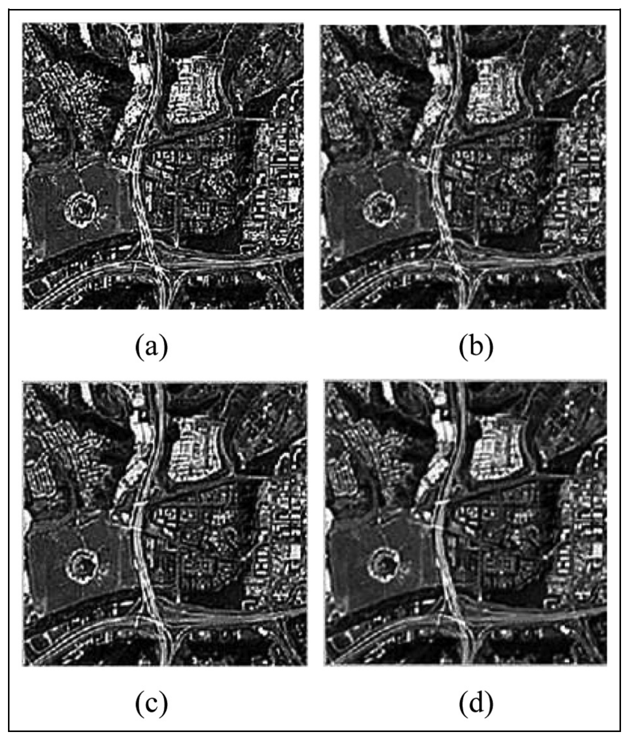

Figure 8. The enhanced images after processing different high-frequency sub-bands: (a) processing the first high-frequency sub-band; (b) processing the second high-frequency sub-band; (c) processing the third high-frequency sub-band; (d) processing all high-frequency sub-bands.

Conclusion

After study NSCT, a new remote sensing image enhancement method using the mean filter and unsharp masking algorithm based on NSCT is proposed by taking advantage of the multidirection, multi-scale and shift-invariance of NSCT. The greater enhancement performance of the proposed method is supported by our experimental results. However, we found that the PSNR and the Q^{AF} of the proposed method are a little lower than the NSCT-UM method. Improvement of the PSNR and the Q^{AF} without reducing definition and contrast in our proposed method will be the focus of future studies.

Declaration of conflicting interest

The authors declare that there is no conflict of interest.

Funding

We are grateful for the financial support by International Cooperative Research and Personnel Training Projects of the Ministry of Education of the People's Republic of China.

References

Backstrom T (2014) Decorrelating MVDR filterbanks using the non-uniform discrete Fourier transform. *IEEE Signal Processing Letters* 22(4): 479–483.

Bhadauria HS and Dewal ML (2014) Analysis of effect of cycle spinning on wavelet-and curvelet-based denoising methods on brain CT images. *Journal of the Chinese Institute of Engineers*, 1–7.

Bin F, Xinyan X and Guozhen S (2011) An efficient mean filter algorithm. In: *IEEE/ICME International Conference on Complex Medical Engineering (CME)*, pp. 466–470.

Brown TJ (2000) An adaptive strategy for wavelet based image enhancement. *Proceedings of the IMVIP*, 67–81.

Buades A, Coll B and Morel J (2005) A review of image denoising algorithms, with a new one. *Multiscale Modeling & Simulation* 4: 490–530.

Cunha AL, Zhou J and Do MN (2005) Nonsubsampled contourilet transform: filter design and applications in denoising. In: *IEEE International Conference on Image Processing*, pp. I-749–52.

Cosman PC, Riskin EA and Gray RM (2014) Combining vector quantization and histogram equalization. *Information Processing and Management*, 28(6).

Da Cunha AL, Zhou J and Do MN (2006) The nonsubsampled contourlet transform: theory, design, and applications. *IEEE Transactions on Image Processing* 15: 3089–3101.

Das S and Kundu MK (2012) NSCT-based multimodal medical image fusion using pulse-coupled neural network and modified spatial frequency. *Medical & Biological Engineering & Computing* 50: 1105–1114.

Demirel H and Anbarjafari G (2011) Image resolution enhancement by using discrete and stationary wavelet decomposition. *IEEE Transactions on Image Processing* 20: 1458–1460.

Di H and Gao D (2014) Gray-level transformation and Canny edge detection for 3D seismic discontinuity enhancement. *Computers & Geosciences* 72: 192–200.

Do MN and Vetterli M (2002a) Contourlets: a directional multiresolution image representation. *International Conference on Image Processing* 1: I-357–I-360.

Do MN and Vetterli M (2002b) Contourlets: a new directional multiresolution image representation. *Conference Record of the Thirty-Sixth Asilomar Conference on Signals, Systems and Computers*, pp. 497–501.

Do MN and Vetterli M (2005) The contourlet transform: an efficient directional multiresolution image representation. *IEEE Transactions on Image Processing* 14: 2091–2106.

Ganasala P and Kumar V (2014) CT and MR image fusion scheme in nonsubsampled contourlet transform domain. *Journal of Digital Imaging* 27(3): 407–418.

Gelman R, Martinez-Perez ME, Vanderveen DK, et al. (2005) Diagnosis of plus disease in retinopathy of prematurity using retinal image multiscale analysis. *Investigative Ophthalmology & Visual Science* 46: 4734–4738.

Henan W, Guang Y, Zhonglin X, et al. (2011) Remote sensing image enhancement method based on multi-scale retinex. *2011 International Conference on Information Technology, Computer Engineering and Management Sciences (ICM)*, pp. 15–18.

Hirschmugl CJ and Gough KM (2012) Fourier transform infrared spectrochemical imaging: review of design and applications with a focal plane array and multiple beam synchrotron radiation source. *Applied Spectroscopy* 66: 475–491.

İlk HG, Jane O and İlkÖ (2011) The effect of Laplacian filter in adaptive unsharp masking for infrared image enhancement. *Infrared Physics & Technology* 54: 427–438.

Iqbal MZ, Ghafoor A, Siddiqui AM, et al. (2014) Dual-tree complex wavelet transform and SVD based medical image resolution enhancement. *Signal Processing* 105: 430–437.

Jain AK (1989) *Fundamentals of Digital Image Processing*. Englewood Cliffs, NJ: Prentice-Hall.

Kumar BKS (2013) Image denoising based on non-local means filter and its method noise thresholding. *Signal, Image and Video Processing* 7: 1211–1227.

Kwok N and Shi H (2014) Design of unsharp masking filter kernel and gain using particle swarm optimization. In: *2014 7th International Congress on Image and Signal Processing (CISP)*, pp. 217–222.

Li S and Zhanli S (2014) Image reconstruction using WTA-ICA model in contourlet transform domain. In *3rd International Conference on Computer Science and Service System*. Bangkok: Atlantis Press.

Li Z, Yu L, Trzasko JD, et al. (2014) Adaptive nonlocal means filtering based on local noise level for CT denoising. *Medical Physics* 41: 011908.

Liu H, Yang C, Pan N, et al. (2010) Denoising 3D MR images by the enhanced non-local means filter for Rician noise. *Magnetic Resonance Imaging* 28: 1485–1496.

Liu L, Chen CP, Zhou Y, et al. (2015) A new weighted mean filter with a two-phase detector for removing impulse noise. *Information Sciences*.

Mallat SG (1989) A theory for multiresolution signal decomposition: the wavelet representation. *IEEE Transactions on Pattern Analysis and Machine Intelligence* 11(7): 674–693.

Men GZ, Yang JL and Zhao J (2010) Fuzzy contrast enhancement for remote sensing image based on fuzzy set in nonsubsampled contourlet domain. In: *2010 International Conference on Machine Learning and Cybernetics (ICMLC)*, pp. 735–740.

Nezhadarya E and Shamsollahi MB (2006) Image contrast enhancement by contourlet transform. In: *48th International Symposium ELMAR-2006 focused on Multimedia Signal Processing and Communications*, pp. 81–84.

Polesel A, Ramponi G and Mathews V J (2000) Image enhancement via adaptive unsharp masking. *IEEE Transactions on Image Processing* 9: 505–510.

Pu X, Jia Z, Wang L, et al. (2014) The remote sensing image enhancement based on nonsubsampled contourlet transform and unsharp masking. *Concurrency and Computation: Practice and Experience* 26: 742–747.

Swaminathan A, Ramapackiam SSK, Thiraviam T, et al. (2013) Contourlet transform-based sharpening enhancement of retinal images and vessel extraction application. *Biomedizinische Technik/Biomedical Engineering* 58: 87–96.

Srivastava R and Khare A (2015) Medical image fusion using local energy in nonsubsampled contourlet transform domain. In: *Computational Vision and Robotics*. Delhi: Springer India, pp. 29–35.

Thien HT, Le BV, Lee S, et al. (2014) Using weighted dynamic range for histogram equalization to improve the image contrast. *EURASIP Journal on Image and Video Processing*, 1–17.

Vijayan M, Josemartin MJ and Geetharanjin PR (2014) Image resolution enhancement using undecimated double density dual tree wavelet transform. In: *2014 International Conference on Contemporary Computing and Informatics (IC3I)*, pp. 734–739).

Weisstein EW (2015) Fast Fourier transform. From MathWorld – A Wolfram Web Resource. http://mathworld.wolfram.com/FastFourierTransform.html

Xydeas CS and Petrović V (2000) Objective image fusion performance measure. *Electronics Letters* 36(4): 308–309.

Yang S, Oh J and Park Y (2003) Contrast enhancement using histogram equalization with bin underflow and bin overflow. In: *International Conference on Image Processing*, vol. 1, pp. I-881–4.

Yin M, Liu W, Zhao X, et al. (2013) Image denoising using trivariate prior model in nonsubsampled dual-tree complex contourlet transform domain and non-local means filter in spatial domain. *Optik-International Journal for Light and Electron Optics* 124(24): 6896–6904.

Yu R (2012) Shift-variance analysis of generalized sampling processes. *IEEE Transactions on Signal Processing* 60: 2840–2850.